fluids

Article

Density, Viscosity, and Excess Properties of Ternary Aqueous Mixtures of MDEA + MEA, DMEA + MEA, and DEEA + MEA

Sumudu S. Karunarathne, Dag A. Eimer, Klaus J. Jens and Lars E. Øi *

Faculty of Technology, Natural Sciences and Maritime Studies, University of South-Eastern Norway, Kjølnes Ring 56, 3901 Porsgrunn, Norway; sumuduunimrt@gmail.com (S.S.K.); Dag.A.Eimer@usn.no (D.A.E.); Klaus.J.Jens@usn.no (K.J.J.)

* Correspondence: lars.oi@usn.no; Tel.: +47-35-575-141

Received: 3 January 2020; Accepted: 10 February 2020; Published: 19 February 2020

Abstract: This study presents the measured densities and viscosities of three ternary aqueous mixtures of tertiary and primary amines. The tertiary amines of N-methyldiethanolamine (MDEA), dimethylethanolamine (DMEA), diethylethanolamine (DEEA), and the primary amine monoethanolamine (MEA) at different concentrations (mass%) were mixed to prepare the liquid mixtures. The excess molar volume V^E of the mixtures was analyzed using measured densities to acquire a better understanding of the molecular packing and intermolecular interactions in the mixtures. The excess free energy of activation ΔG^{E*} and excess entropy of activation ΔS^{E*} for viscous flow were determined from the measured viscosities by implementing the theory of rate processes of Eyring. Correlations based on the Redlich–Kister type polynomial were adopted to correlate the excess properties V^E and ΔG^{E*} as a function of the amine mole fraction and temperature. The results showed that the correlations were able to represent the measured data with satisfactory accuracies for engineering calculations.

Keywords: density; viscosity; MDEA; DMEA; DEEA; excess property; Redlich–Kister

1. Introduction

The chemical absorption of CO_2 into aqueous alkanolamines is a mature technology that has been used for decades in the natural gas industry. The solvent-based commercial scale post-combustion CO_2 capture plants are generally operated with 15–20 mass% aqueous monoethanolamine (MEA), 30 mass% aqueous MEA, KS-1 based on sterically hindered amines, and DC-103 from Shell Cansolv (50 mass% amine and 50 mass% H_2O) [1–3]. Bernhardsen and Knuutila [4] reviewed the potential amine solvents for CO_2 absorption process by considering the absorption capacity, cyclic capacity, and pKa. The studies performed on 3-amino-1-propanol (3A1P) [5,6] and diethylenetriamine (DETA) [7,8] stated the possibilities of using them as solvents in post-combustion CO_2 capture. The applicability of this technology to post-combustion CO_2 capture is challenging owing to the economic feasibility of the process due to the high-energy penalty in the CO_2 stripping. MEA is a primary amine that shows a high CO_2 absorption rate, which is promising for the process. The main disadvantage of MEA is that it requires a high amount of energy to release CO_2 during the stripping. Tertiary amines like N-methyldiethanolamine (MDEA), dimethylethanolamine (DMEA), and diethylethanolamine (DEEA) have a low heat of reaction, which lowers the energy requirement in the stripping process [9–11]. MDEA is traditionally used for CO_2 removal at high pressures. It is normally not used for CO_2 removal at atmospheric pressure [12]. The MDEA solutions are used for the selective removal of H_2S from gas streams like natural gases, synthesis gases from the gasification of coal and heavy oils, and tail gases from sulphur plants that contain both CO_2 and H_2S [13,14]. In addition to the selective removal of H_2S, several advantages of MDEA over primary and secondary amines were reported, such as low vapor pressure, high CO_2 absorption capacity, high resistance to degradation, and fewer corrosion problems [15,16]. The low CO_2 absorption rate of tertiary amines makes it inefficient to use them alone with H_2O as a solvent in the absorption–desorption process to deal with gas streams with low CO_2 concentrations. The work performed by Kim and Savage [17] on reaction kinetics of CO_2 absorption in aqueous DEEA claimed that DEEA has a higher reaction rate than MDEA. Alongside the results found by Henni et al. [18] on kinetics of DMEA, it was observed that DMEA and DEEA have a higher absorption performance compared to MDEA [9]. Chakravarty et al. [19] demonstrated that CO_2 absorption can be enhanced by adding a primary or secondary amine to the tertiary amine without changing the stripping characteristics. Studies have been performed to investigate the performance of aqueous blends of tertiary and primary amines in CO_2 absorption [9,20–22]. Conway et al. [21] showed improvements in the cyclic capacity of DMEA + MEA + H_2O and DEEA + MEA + H_2O mixtures compared to aqueous MEA mixtures.

Physical properties, such as the density and viscosity of solvents, are essential for engineering calculations when performing mathematical modelling and simulations for the sizing of process equipment. The density and viscosity are required in many mass and heat transfer correlations that are used in the designing of absorbers, strippers, and heat exchangers in the process. Further properties are useful in flow calculations to select material transfer equipment like pumps and valves. The density and viscosity data of some MDEA + MEA + H_2O mixtures have been reported in literature sources [23–25]. For the mixtures of DMEA + MEA + H_2O and DEEA + MEA + H_2O, literature for measured properties are scarce [21].

In this study, the measurements of density and viscosity of three different aqueous tertiary and primary amines mixtures of MDEA (1) + MEA (2) + H_2O (3), DMEA (1) + MEA (2) + H_2O (3), and DEEA (1) + MEA (2) + H_2O (3) at different amine concentrations and temperatures were performed. The excess properties of molar volume, viscosity, and free energy of activation and entropy for viscous flow were determined to examine the molecular structure and interactions in the mixtures. Finally, the data were fitted to the density and viscosity correlations available in the literature and parameters were determined via regression. The accuracy of the data fitting was examined through average absolute relative deviation (*AARD* (%)) and absolute maximum deviation (*AMD*).

2. Materials and Methods

2.1. Material Description

Table 1 lists the materials that were used in this study. Liquid mixtures of aqueous tertiary and primary amines of MDEA + MEA + H_2O, DMEA + MEA + H_2O, and DEEA + MEA + H_2O were prepared on the mass basis using a balance, model: XS-403S from Mettler Toledo (Greifensee, Switzerland) with a resolution of 1 mg. Amines were used without further purification and dissolved with deionized (resistivity: 18.2 MΩ cm) and degassed water from a rotary evaporator (Rotavapor R-210, Buchi, Flawil, Switzerland).

Table 1. Materials used in this study.

Chemical Name	CAS No.	Source	Purity
MDEA	105-59-9	Merck Schuchardt OHG, Hohenbrunn, Germany	≥98%
DMEA	108-01-0	Alfa Aesar, Kandel, Germany	≥99
DEEA	100-37-8	Sigma-Aldrich, Darmstadt, Germany	≥99.5%
MEA	141-43-5	Sigma-Aldrich, Darmstadt, Germany	≥99.5% (GC) [a]

[a] GC: Gas chromatography.

2.2. Density Measurement

Density of the mixtures was measured using a density meter of DMA 4500 from Anton Paar (Graz, Austria) under atmospheric conditions. DMA 4500 has a temperature controller with an accuracy of ±0.03 K and the accuracy of the density measurement is ±0.05 kg m^{-3}. A liquid sample with a volume of approximately 5 mL was used to take the density reading and a new sample was fed into the U-tube for density measurements at each temperature and composition. In order to check the reliability of the instrument, a density check was performed frequently at 293.15 K using degassed deionized water. As suggested by the manufacturer, the density check is accepted when the deviations between the experimental and stored reference density data is smaller than 0.1 kg m^{-3}. For deviations greater than 0.1 kg m^{-3}, a calibration was performed using both air and degassed deionized water at 293.15 K as per the instruction given by the manufacturer. The density of water was measured at different temperatures and compared with the literature data from the International Association for the Properties of Water and Steam (IAPWS) [26]. The comparison showed that the deviation of the measured density of water was less than 0.01%, which was acceptable.

2.3. Viscosity Measurement

A double-gap rheometer (pressure cell XL, Anton Paar, Graz, Austria) Physica MCR 101 was used for the dynamic viscosity measurements of the aqueous amine mixtures. A liquid sample of 7 mL in volume was transferred using a syringe in the space occupied between the rotating and fixed cylinders in the pressure cell. For the viscosity measurements at temperatures higher than 303.15 K, the internal temperature controller with an accuracy of ±0.03 K was used to maintain different temperatures up to 363.15 K. An external cooling system Viscotherm VT 2 (Anton Paar, Graz, Austria) with an accuracy of ±0.02 K was adopted to acquire precise measurements for the temperature range from 293.15 K to 303.15 K. Following the instructions provided by Anton Paar, an air check and motor adjustment were performed prior to the experiments. The accuracy of the torque measurement is given by the manufacturer as max (0.2 μNm; 0.5%) and the repeatability of the viscosity measurements is ±0.008 mPa s. Further, a standard viscosity solution S3S from Paragon Scientific Ltd. (Prenton, United Kingdom) was used to calibrate the measuring system. The viscosity of the standard viscosity fluid was measured at specific temperatures suggested by the supplier and was compared with the reference data to record deviations. The measured viscosities were corrected for these deviations obtained during the calibration. The experiments were conducted at atmospheric pressure (1 atm).

2.4. Experimental Uncertainty

Several uncertainty sources of material purity $u(p)$, temperature measurement $u(T)$, weight measurement $u(w)$, and repeatability $u(rep)$ were taken into account to determine the combined standard uncertainty of density and viscosity measurements of aqueous amine mixtures.

For the uncertainty of density measurement, the specified standard uncertainties were $u(p)$ = ±0.003, $u(T)$ = ±0.012 K, $u(w)$ = ±2 × 10^{-4} kg, and $u(rep)$ = ±0.13 kg m^{-3}. The maximum gradient of density against temperature, $\partial\rho/\partial T$, was found to be 0.88 kg m^{-3} K^{-1} and the corresponding uncertainty in ρ, $(\partial\rho/\partial T)\cdot u(T)$, was determined to be ±0.0106 kg m^{-3}. The combined standard uncertainty for the density measurement was calculated as described in the Guide to the Expression of Uncertainty in Measurement [27,28] by considering all mentioned uncertainty sources to be $u(\rho)$ = ±2.97 kg m^{-3}. Then, the combined expanded uncertainty of the density measurement $U(\rho)$ was found to be ±5.94 kg m^{-3} (level of confidence $=$ 0.95).

In the uncertainty of viscosity measurement, specified standard uncertainties for the uncertainty sources were $u(p)$ = ±0.003, $u(T)$ = ±0.012 K, $u(w)$ = ±2 × 10^{-4} kg, and $u(rep)$ = ±0.008 mPa s. The combined standard uncertainty for the viscosity measurement was calculated to be $u(\eta)$ = ±0.008 mPa s. Then, the combined expanded uncertainty of the viscosity measurement $U(\eta)$ was found to be ±0.016 mPa s (level of confidence $=$ 0.95).

3. Results

3.1. Density and Excess Molar Volume

The density of pure MDEA, DEEA, DMEA, and MEA are available in the literature. The measured densities of pure amines over a temperature range from 293.15 K to 343.15 K are listed in Table 2 with the relevant literature data and references. The measured density in this work is in good agreement with values reported in literature, which indicates the density meter was properly calibrated during the experiments.

Table 2. Densities ρ/kg m^{-3} of pure amines MDEA, DMEA and DEEA.

Amine	**T (K)**	**This Work**	**Literature**		
			Pinto et al. [29]	**Hawrylak et al. [30]**	**Maham et al. [31]**
MDEA	293.15	1040.6	1040.12		
	298.15	1036.8		1036.88	1035.9
	303.15	1033.2			1032.0
	308.15	1029.4		1029.01	
	313.15	1025.6	1024.74		1024.45
	318.15	1021.8		1022.64	
	323.15	1018.0	1017.27		1016.66
	328.15	1014.1			
	333.15	1010.3	1009.56		1009.00
	338.15	1006.4			
	343.15	1002.5			1001.24
	T/(K)	**This Work**	**Literature**		
			Maham et al. [32]	**Hawrylak et al. [30]**	**Bernal-García et al. [33]**
DMEA	293.15	887.3			887.816
	298.15	883.0	882.57	883.34	883.578
	303.15	878.8	878.35		879.315
	308.15	874.5		875.46	875.017
	313.15	870.1	869.86		870.686
	318.15	865.8		867.28	866.316
	323.15	861.4			861.902
	328.15	856.9			857.460
	333.15	852.5	851.89		852.965
	338.15	847.9			848.423
	343.15	843.3			843.844
	T/(K)	**This Work**	**Literature**		
			Zhang et al. [34]	**Hawrylak et al. [30]**	**Pinto et al. [29]**
DEEA	293.15	884.3	884.20		
	298.15	879.7	879.54	879.52	879.47
	303.15	875.1	874.82		
	308.15	870.4		871.40	
	313.15	865.8	865.56		865.54
	318.15	861.1		861.82	
	323.15	856.3			856.12
	328.15	851.5			
	333.15	846.7			846.61
	338.15	841.9			
	343.15	837.1			837.03

The measured densities of MDEA + MEA + H_2O, DMEA + MEA + H_2O, and DEEA + MEA + H_2O mixtures over different amine concentrations (mass% of amine) and temperatures from 293.15 K to 343.15 K are listed in Tables 3–5, respectively. For the density of MDEA + MEA + H_2O mixtures, the density increased with the increase of the MDEA concentration in the mixture. Moreover, for the

DMEA + MEA + H_2O and DEEA + MEA + H_2O mixtures, the density increased with the decrease of the DMEA and DEEA concentration in the mixtures.

Table 3. Densities ρ (kg m^{-3}) and excess molar volume V^E (m^3 mol^{-1}) of MDEA (1) + MEA (2) + H_2O (3) mixtures.

Mixtures	**MDEA/MEA**							
(Mass%/Mass%)	**15/15**		**20/10**		**25/5**		**30/0**	
[a]x_1/x_2	**0.0296/0.0577**		**0.0398/0.0388**		**0.0502/0.0196**		**0.0609/0.0000**	
T (K)	ρ	V^E (×10^6)	ρ	V^E (×10^6)	ρ	V^E (×10^6)	ρ	V^E (×10^6)
293.15	1019.7	−0.292	1022.1	−0.321	1024.5	−0.351	1026.9	−0.382
298.15	1017.6	−0.288	1019.9	−0.317	1022.3	−0.347	1024.7	−0.377
303.15	1015.3	−0.284	1017.6	−0.313	1020.05	−0.342	1022.4	−0.371
308.15	1012.8	−0.282	1015.2	−0.310	1017.6	−0.339	1019.9	−0.367
313.15	1010.3	−0.281	1012.6	−0.308	1015.0	−0.336	1017.3	−0.364
318.15	1007.6	−0.280	1009.9	−0.306	1012.2	−0.332	1014.6	−0.361
323.15	1004.8	−0.278	1007.1	−0.304	1009.3	−0.329	1011.7	−0.357
328.15	1001.9	−0.277	1004.1	−0.302	1006.3	−0.324	1008.7	−0.354
333.15	998.8	−0.276	1000.9	−0.297	1003.2	−0.323	1005.6	−0.350
338.15	995.6	−0.273	997.5	−0.288	999.7	−0.312	1002.3	−0.346
343.15	991.7	−0.257	993.1	−0.261	995.4	−0.287	998.7	−0.336

[a] x = mole fraction.

Table 4. Densities ρ (kg m^{-3}) and excess molar volume V^E (m^3 mol^{-1}) of DMEA (1) + MEA (2) + H_2O (3) mixtures.

Mixtures	**DMEA/MEA**							
(Mass%/Mass%)	**15/15**		**20/10**		**25/5**		**30/0**	
[a]x_1/x_2	**0.0391/0.0571**		**0.0525/0.0383**		**0.0660/0.0193**		**0.0797/0.0000**	
T (K)	ρ	V^E (×10^6)	ρ	V^E (×10^6)	ρ	V^E (×10^6)	ρ	V^E (×10^6)
293.15	1001.9	−0.463	998.4	−0.550	994.4	−0.626	990.9	−0.715
298.15	999.6	−0.460	995.9	−0.545	991.8	−0.620	988.1	−0.707
303.15	996.7	−0.448	993.2	−0.539	989.0	−0.613	985.2	−0.698
308.15	994.4	−0.453	990.5	−0.536	986.1	−0.608	982.3	−0.693
313.15	991.6	−0.452	987.6	−0.533	983.1	−0.603	979.2	−0.687
318.15	988.7	−0.450	984.6	−0.531	980.0	−0.600	975.9	−0.682
323.15	985.5	−0.444	981.4	−0.528	976.8	−0.596	972.6	−0.678
328.15	982.5	−0.447	978.0	−0.523	973.4	−0.594	969.2	−0.674
333.15	979.3	−0.448	974.6	−0.520	970.0	−0.591	965.7	−0.671
338.15	975.7	−0.442	971.1	−0.517	966.4	−0.589	962.0	−0.668
343.15	972.4	−0.445	967.4	−0.511	962.8	−0.589	958.4	−0.669

[a] x = mole fraction.

Table 5. Densities ρ (kg m^{-3}) and excess molar volume V^E (m^3 mol^{-1}) of DEEA (1) + MEA (2) + H_2O (3) mixtures.

Mixtures	**DEEA/MEA**							
(Mass%/Mass%)	**15/15**		**20/10**		**25/5**		**30/0**	
[a]x_1/x_2	**0.0301/0.0577**		**0.0404/0.0388**		**0.0510/0.0196**		**0.0618/0.0000**	
T (K)	ρ	V^E (×10^6)	ρ	V^E (×10^6)	ρ	V^E (×10^6)	ρ	V^E (×10^6)
293.15	1002.3	−0.489	998.4	−0.575	994.2	−0.654	989.6	−0.724
298.15	999.8	−0.484	995.7	−0.568	991.4	−0.645	986.5	−0.711
303.15	997.1	−0.479	992.9	−0.561	988.4	−0.636	983.4	−0.702
308.15	994.3	−0.476	990.0	−0.556	985.3	−0.629	980.2	−0.693
313.15	991.4	−0.473	986.9	−0.551	982.1	−0.623	976.9	−0.684
318.15	988.5	−0.471	983.7	−0.547	978.8	−0.617	973.4	−0.677

323.15	985.1	−0.464	980.5	−0.544	975.3	−0.611	969.8	−0.669
328.15	981.8	−0.462	977.1	−0.541	971.8	−0.606	966.2	−0.663
333.15	978.5	−0.459	973.6	−0.538	968.2	−0.602	962.4	−0.657
338.15	974.4	−0.443	970.0	−0.535	964.3	−0.595	958.5	−0.651
343.15	971.1	−0.448	966.2	−0.529	960.4	−0.589	954.6	−0.645

[a] x = mole fraction.

The excess molar volume V^E of the mixtures were determined using the molar volume of the mixture and pure components as follows:

$$V^E = V - \sum_{i=1}^{n} x_i V_i^0, \tag{1}$$

where V, V_i^0, V^E, and x_i refer to the molar volume of the mixture, molar volume of the pure component, excess molar volume of the mixture, and mole fraction, respectively. Here, $n = 3$ to represent the ternary mixture and subscripts are as follows: $i = 1$ for the tertiary amine, $i = 2$ for the primary amine (MEA), and $i = 3$ for H_2O.

The calculated V^E from Equation (1) for MDEA + MEA + H_2O, DMEA + MEA + H_2O, and DEEA + MEA + H_2O mixtures are given in Tables 3–5, respectively. The following correlation was adopted to correlate the density data at different amine concentrations and temperatures. Redlich–Kister [35] polynomials are one of the most common approaches toward correlating the excess properties of binary mixtures because polynomial expressions are simple and easy to understand. Here, it was assumed that excess molar volume of a ternary mixture as a sum of excess molar volumes from different binary pairs, as given in Equation (3). The binary mixture polynomial shown in Equation (4) was extended by adding ternary coefficients for the ternary mixture with a temperature dependency, as described in Equation (5). Finally, the density was determined as follows:

$$\rho = \frac{\sum_{i=1}^{n} x_i M_i}{V^E + \sum_{i=1}^{n} \frac{x_i M_i}{\rho_i}}, \tag{2}$$

where ρ, ρ_i, V^E, x_i, and M_i are the density of the mixture, density of the pure amine, excess molar volume of the mixture, mole fraction, and molecular weight of the pure component, respectively. The subscripts are as follows: $i = 1$ for tertiary amine, $i = 2$ for primary amine (MEA), and $i = 3$ for H_2O.

$$V^E = V_{12}^E + V_{23}^E + V_{13}^E, \tag{3}$$

$$V_{jk}^E = x_j x_k \sum_{i=0}^{n} A_i \left(x_j - x_k\right)^i, \tag{4}$$

$$A_i = a + b(T) + c(T)^2, \tag{5}$$

where A_i are pair parameters and are assumed to be temperature dependent.

Other correlations have been suggested for the excess molar volume of ternary mixtures were reported by Domínguez et al. [36] and Samanta and Bandyopadhyay [37]. References [38–40] suggested correlations for CO_2-loaded solutions, but in this work, emphasis is on non-loaded aqueous amine mixtures.

The accuracy of the proposed correlation for the fitting of measured densities was examined through the average absolute relative deviation (*AARD* (%)) and the absolute maximum deviation (*AMD*) as defined in Equations (6) and (7), respectively.

Average absolute relative deviation:

$$AARD\ (\%) = \frac{100\%}{N} \sum_{i=1}^{N} \left| \frac{Y_i^E - Y_i^C}{Y_i^E} \right|, \tag{6}$$

and the absolute maximum deviation:

$$AMD = MAX\left|Y_i^E - Y_i^C\right| \tag{7}$$

where N, Y_i^E, and Y_i^C indicate the number of data points, the measured property, and the calculated property, respectively.

Figure 1 shows a comparison between the measured versus correlated density data for aqueous amine mixtures. The study reveals that the proposed correlation fits the density data with an acceptable accuracy. The calculated parameters for the excess volume V^E correlation are given in Tables 6–8. The reported *AARD* and *AMD* for the density correlation of MDEA + MEA + H_2O, DMEA + MEA + H_2O, and DEEA + MEA + H_2O are listed in Table 9. The regression performed with a linear temperature dependency in Equation (5) revealed a 13% increase of *AARD* for MDEA + MEA + H_2O mixtures, as given in Table 9. This indicated that the proposed correlation gave a better fit for the density data.

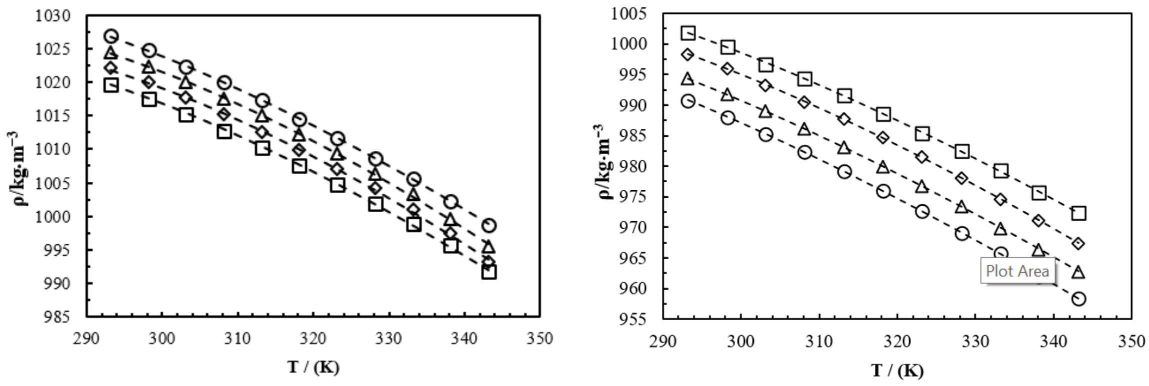

(**a**) Experiment; "□" 15%, "△" 20%, "◇" 25%, "○" 30% (mass% MDEA), correlation; "– – –".

(**b**) Experiment; "□" 15%, "△" 20%, "◇" 25%, "○" 30% (mass% DMEA), correlation; "– – –".

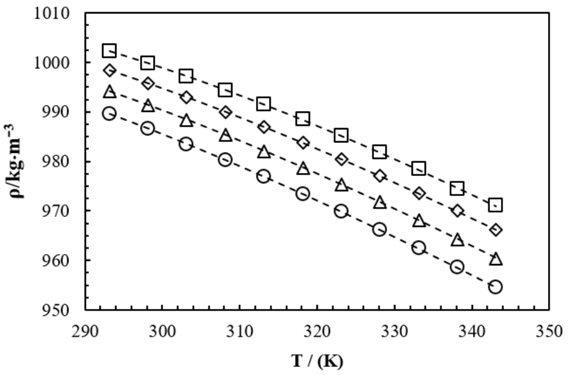

(**c**) Experiment; "□" 15%, "△" 20%, "◇" 25%, "○" 30% (mass% DEEA), correlation; "– – –".

Figure 1. Density of: (**a**) MDEA + MEA + H_2O, (**b**) DMEA + MEA + H_2O, and (**c**) DEEA + MEA + H_2O mixtures in the temperature range 293.15 K–343.15 K.

Table 6. Binary parameters A_0, A_1, and A_2 of the equation $V_{jk}^E = x_j x_k \sum_{i=0}^{n} A_i (x_j - x_k)^i$ for the excess molar volume of MDEA (1) + MEA (2) + H_2O (3).

Parameters		**Binary Pair**		
		MDEA + MEA	**MEA + H_2O**	**MDEA + H_2O**
A_0	a	−5740.7862	110.3506	0.7103
	b	−9.4267	0.5623	0.0984
	c	−6.0994	0.7119	0.6020
A_1	a	47,728.6381	−91.5628	0.5925

	b	82.8194	0.5242	0.3620
	c	70.3044	0.4374	0.6230
A_2	a	−41,5410.0557	70.3808	−0.2463
	b	−724.8059	0.3897	0.2846
	c	−601.8188	−0.0807	−0.0710

Table 7. Binary parameters A_0, A_1, and A_2 of the equation $V_{jk}^E = x_j x_k \sum_{i=0}^{n} A_i (x_j - x_k)^i$ for the excess molar volume of DMEA (1) + MEA (2) + H_2O (3).

Parameters		Binary Pair		
		DMEA + MEA	MEA + H_2O	DMEA + H_2O
A_0	a	1236.6194	−29.4723	−0.2082
	b	1.2313	0.1074	0.3237
	c	−4.8869	0.1673	0.3986
A_1	a	−10,260.3999	24.7205	0.3942
	b	−18.2970	0.9283	0.5201
	c	36.5240	0.3256	0.7509
A_2	a	66,361.3723	−16.8614	0.7635
	b	110.1435	0.8558	0.1605
	c	−240.1085	0.4951	0.3292

Table 8. Binary parameters A_0, A_1, and A_2 of the equation $V_{jk}^E = x_j x_k \sum_{i=0}^{n} A_i (x_j - x_k)^i$ for the excess molar volume of DEEA (1) + MEA (2) + H_2O (3).

Parameters		Binary Pair		
		DEEA + MEA	MEA + H_2O	DEEA + H_2O
A_0	a	1499.9879	−31.3131	−0.3593
	b	−7.4459	0.5442	0.2384
	c	1.3969	0.0633	0.3485
A_1	a	−12,608.1516	24.6564	−0.4664
	b	68.6619	0.4921	0.7533
	c	−19.8546	0.5935	0.6335
A_2	a	107,748.3754	−15.3309	−0.0644
	b	−588.5102	0.2714	0.5491
	c	156.7816	0.5154	0.2691

Table 9. Average absolute relative (*AARD*) and absolute maximum (*AMD*) deviations calculated based on the correlation proposed from Equations (2)–(5).

Mixture	*AARD* (%)	*AMD* (kg m^{-3})
MDEA + MEA + H_2O	0.013	0.4
DMEA + MEA + H_2O	0.004	0.3
DEEA + MEA + H_2O	0.005	0.3

The supplementary materials provide the information of the used MATLAB program for the calculation of parameters involve in density correlation.

The excess molar volume V^E of the ternary mixtures showed a negative sign for the considered amine concentrations and temperatures. The negative sign of V^E can be explained by the intermolecular packing effect and strong intermolecular interactions, such as H-bonding between unlike molecules. The relatively small structures of MEA and H_2O compared to MDEA, DMEA, and DEEA could help to pack molecules efficiently, which resulted in the decrease of the mixture volume. In addition, the formation of H-bonds among the tertiary amines, MEA, and H_2O could also lead the volume of tertiary mixtures to show a negative deviation of V^E. The highest negative values were reported in the mixtures with a 0 mass% MEA concentration. The V^E increased with the increasing of MEA concentration in the mixtures. Further, V^E increased with the increase of temperature. At high temperatures, the increase of the energy of molecular motion weakens the interaction strength of H-bonds and inhibits the packing effect by leading to an increase of volume [41,42].

3.2. Viscosity and Excess Free Energy of Activation for Viscous Flow

Table 10 provides an overview of the measured viscosities of pure MDEA, DMEA, and DEEA from this study and literature at different temperatures from 293.15 K to 363.15 K. As shown in Figure 2, the measured viscosities in this work were in good agreement with data in the literature. It indicated that the measuring system was properly calibrated during the viscosity measurements. The measured viscosities for MDEA + MEA + H_2O, DMEA + MEA + H_2O, and DEEA + MEA + H_2O mixtures are listed in Tables 11–13, respectively, with the relevant concentrations and temperatures. For the mixtures, the viscosity increased with the increase of the tertiary amine concentration and the viscosity decreased with the increase of temperature.

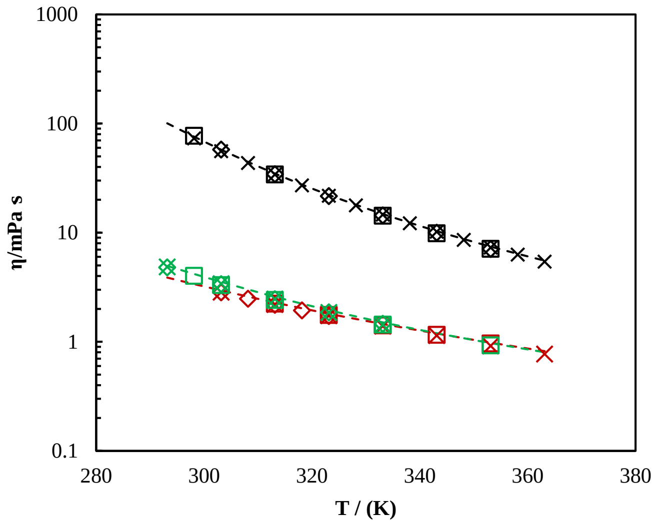

Figure 2. Viscosity of MDEA: "– – –"—this work; "□"—Teng et al. [43]; "◇"—Li and Lie [24]; "x"—Kummamuru et al. [44]. Viscosity of DMEA: "– – –"—this work; "□"—Bernal-García et al. [33]; "◇"—Chowdhury et al. [45]; "x"—DiGuilio et al. [46]. Viscosity of DEEA: "– – –"—this work; "□"—Maham et al. [32]; "◇"—Chen et al. [47]; "x"—Ma et al. [48].

Table 10. Viscosities η (mPa s) of pure amines MDEA, DMEA, and DEEA.

Amine	T (K)	This Work	Literature		
			Teng et al. [43]	Li and Lie [24]	Kummamuru et al. [44]
MDEA	293.15	100.630			
	298.15	75.775	77.19		73.10
	303.15	57.658		57.860	55.89
	308.15	44.483			43.45
	313.15	34.786	34.11	34.309	34.15
	318.15	27.575			27.15
	323.15	22.145		21.672	21.82
	328.15	18.024			17.79
	333.15	14.820	14.30	14.386	14.63
	338.15	12.319			12.20
	343.15	10.325	9.849	9.979	10.21

	348.15	8.735			8.60
	353.15	7.444	7.115	7.086	7.31
	358.15	6.395			6.29
	363.15	5.535			5.43
	T (K)	**This Work**	**Literature**		
			Bernal-García et al. [33]	**Chowdhury et al. [45]**	**DiGuilio et al. [46]**
DMEA	293.15	3.879			
	298.15	3.381			
	303.15	2.959		2.835	2.849
	308.15	2.595		2.485	
	313.15	2.288	2.238	2.186	2.194
	318.15	2.028		1.938	
	323.15	1.807	1.756	1.723	1.734
	328.15	1.618			
	333.15	1.455	1.413		1.394
	338.15	1.315			
	343.15	1.190	1.156		1.140
	348.15	1.078			
	353.15	0.981	0.963		0.916
	358.15	0.896			
	363.15	0.820			0.773
	T/(K)	**This Work**	**Literature**		
			Maham et al. [32]	**Chen et al. [47]**	**Ma et al. [48]**
DEEA	293.15	4.950		4.81	4.848
	298.15	4.174	4.022		
	303.15	3.536	3.308	3.37	3.410
	308.15	3.010			
	313.15	2.579	2.414	2.46	2.466
	318.15	2.230			
	323.15	1.943		1.86	1.855
	328.15	1.704			
	333.15	1.503	1.435	1.46	1.431
	338.15	1.337			
	343.15	1.196			
	348.15	1.076			
	353.15	0.971	0.925		
	358.15	0.881			
	363.15	0.800			

Table 11. Viscosities η (mPa s) and viscosity deviation η^E (mPa s) of MDEA (1) + MEA (2) + H₂O (3) mixtures.

Mixtures	**MDEA/MEA**							
(Mass%/Mass%)	**15/15**		**20/10**		**25/5**		**30/0**	
$^a x_1/x_2$	**0.0296/0.0577**		**0.0398/0.0388**		**0.0502/0.0196**		**0.0609/0.0000**	
T/(K)	η	η^E	η	η^E	η	η^E	η	η^E
293.15	3.263	−1.976	3.436	−2.400	3.581	−2.863	3.712	−3.352

298.15	2.780	−1.337	2.917	−1.635	3.034	−1.961	3.136	−2.311
303.15	2.385	−0.900	2.496	−1.107	2.593	−1.334	2.673	−1.584
308.15	2.065	−0.599	2.156	−0.744	2.235	−0.904	2.301	−1.082
313.15	1.803	−0.390	1.879	−0.489	1.946	−0.601	1.995	−0.735
318.15	1.588	−0.243	1.654	−0.311	1.709	−0.391	1.748	−0.490
323.15	1.410	−0.141	1.467	−0.185	1.512	−0.244	1.544	−0.318
328.15	1.264	−0.065	1.314	−0.095	1.350	−0.138	1.376	−0.194
333.15	1.140	−0.012	1.184	−0.029	1.215	−0.061	1.236	−0.104
338.15	1.036	0.030	1.075	0.020	1.099	−0.007	1.117	−0.039
343.15	0.947	0.058	0.979	0.051	0.998	0.030	1.017	0.010
348.15	0.867	0.077	0.896	0.075	0.913	0.060	0.930	0.044
353.15	0.797	0.090	0.824	0.092	0.841	0.082	0.853	0.068
358.15	0.741	0.103	0.763	0.104	0.777	0.097	0.790	0.089
363.15	0.712	0.133	0.722	0.126	0.738	0.125	0.747	0.116

^{a}x = mole fraction.

Table 12. Viscosities η (mPa s) and viscosity deviation η^E (mPa s) of DMEA (1) + MEA (2) + H_2O (3) mixtures.

Mixtures	**DMEA/MEA**							
(Mass%/Mass%)	**15/15**		**20/10**		**25/5**		**30/0**	
$^{a}x_1/x_2$	**0.0391/0.0571**		**0.0525/0.0383**		**0.0660/0.0193**		**0.0797/0.0000**	
T/(K)	η	η^E	η	η^E	η	η^E	η	η^E
293.15	3.523	1.130	3.744	1.734	4.079	2.456	4.245	3.013
298.15	2.969	0.978	3.130	1.437	3.389	1.996	3.487	2.398
303.15	2.512	0.832	2.644	1.197	2.848	1.639	2.898	1.928
308.15	2.155	0.718	2.256	1.006	2.410	1.349	2.440	1.571
313.15	1.866	0.624	1.943	0.852	2.064	1.126	2.079	1.296
318.15	1.632	0.547	1.691	0.729	1.790	0.953	1.791	1.081
323.15	1.439	0.482	1.485	0.629	1.565	0.813	1.557	0.909
328.15	1.282	0.430	1.319	0.552	1.386	0.706	1.369	0.776
333.15	1.149	0.386	1.180	0.489	1.235	0.616	1.212	0.666
338.15	1.038	0.351	1.063	0.436	1.111	0.545	1.082	0.578
343.15	0.942	0.318	0.962	0.390	1.001	0.481	0.973	0.507
348.15	0.859	0.291	0.874	0.350	0.906	0.427	0.882	0.448
353.15	0.788	0.267	0.800	0.318	0.827	0.384	0.805	0.401
358.15	0.728	0.248	0.735	0.288	0.761	0.349	0.737	0.360
363.15	0.701	0.257	0.703	0.289	0.711	0.328	0.686	0.333

^{a}x = mole fraction.

Table 13. Viscosities η (mPa s) and viscosity deviation η^E (mPa s) of DEEA (1) + MEA (2) + H_2O (3) mixtures.

Mixtures	**DEEA/MEA**							
(Mass%/Mass%)	**15/15**		**20/10**		**25/5**		**30/0**	
$^{a}x_1/x_2$	**0.0301/0.0577**		**0.0404/0.0388**		**0.0510/0.0196**		**0.0618/0.0000**	
T/(K)	η	η^E	η	η^E	η	η^E	η	η^E
293.15	3.691	1.280	3.963	1.933	4.217	2.575	4.536	3.290
298.15	3.086	1.085	3.281	1.577	3.464	2.063	3.689	2.595
303.15	2.604	0.919	2.746	1.296	2.886	1.675	3.048	2.081
308.15	2.220	0.781	2.325	1.075	2.435	1.378	2.552	1.691
313.15	1.910	0.669	1.991	0.904	2.078	1.147	2.165	1.393
318.15	1.662	0.580	1.726	0.769	1.795	0.967	1.860	1.163

323.15	1.460	0.506	1.507	0.658	1.565	0.823	1.617	0.984
328.15	1.296	0.449	1.330	0.571	1.380	0.710	1.419	0.840
333.15	1.159	0.401	1.182	0.498	1.229	0.621	1.259	0.728
338.15	1.041	0.359	1.057	0.438	1.101	0.547	1.126	0.637
343.15	0.942	0.323	0.953	0.388	0.993	0.484	1.016	0.563
348.15	0.858	0.294	0.874	0.357	0.900	0.431	0.920	0.499
353.15	0.782	0.266	0.797	0.321	0.822	0.388	0.842	0.450
358.15	0.719	0.243	0.730	0.289	0.752	0.349	0.771	0.405
363.15	0.686	0.246	0.691	0.283	0.696	0.320	0.708	0.365

[a] x = mole fraction.

The viscosity deviation of the mixtures was calculated as follows:

$$\eta^E = \eta - \sum_{i=1}^{n} x_i \eta_i^0, \tag{8}$$

where η, η_i^0, η^E, and x_i refer to the viscosity of the mixture, viscosity of the pure component, viscosity deviation of the mixture, and mole fraction, respectively. Here, $n = 3$ represents the ternary mixture and the subscripts are as follows: $i = 1$ for the tertiary amine, $i = 2$ for the primary amine (MEA), and $i = 3$ for H_2O.

The viscosity deviation η^E is a property that provides a qualitative measure of intermolecular interactions between component molecules in a liquid mixture. A negative deviation ($\eta^E < 0$) indicates weak intermolecular interactions, while a positive deviation points out strong intermolecular interactions like H-bonding among unlike molecules in the mixture [42,49]. This method is widely used to analyze binary mixtures and the same analogy is adopted to study ternary mixtures [42]. The MDEA + MEA + H_2O mixtures showed a negative deviation for η^E at temperatures <343.15 K, and η^E gradually increased with increasing temperature. As described by Domínguez et al. [50], the η^E can become negative when intermolecular interactions between the molecules are stronger for the pure compounds than for their mixtures. The gradual increase of η^E with increasing temperature implies that the strength of the interactions between the component molecules in mixtures decreases, which may be attributed to the breaking of the cohesive force in like molecules [51]. The mixtures of DMEA + MEA + H_2O and DEEA + MEA + H_2O showed a positive deviation for η^E for the considered concentrations and temperatures. This revealed the association of strong intermolecular interactions of H-bonds in the mixtures. The increase of temperature resulted in a decrease of η^E owing to weakening of intermolecular interaction between unlike molecules.

Eyring [52] explained that in a liquid at rest, the molecules are constantly undergoing rearrangements. This was elaborated by Bird et al. [53] in terms of one molecule at a time escaping from its cage into an adjacent hole. A cage is an available space for a molecule to vibrate due to the surrounding closely packed neighboring molecules. An energy barrier of height $\Delta G^*/N_A$ represents the cage in which ΔG^* and N_A are the free energy of activation for viscous flow and Avogadro's number, respectively.

The dynamic viscosity model for liquids found by Eyring [52] is given as follows:

$$\eta = \frac{hN_A}{V} exp\left(\frac{\Delta G^*}{RT}\right), \tag{9}$$

where η, V, h, N_A, R, T, and ΔG^* refer to the viscosity, molar volume, Planck's constant, Avogadro's number, gas constant, temperature, and free energy of activation for viscous flow, respectively.

Equations (10) and (11) enable the determination of the excess free energy of activation for viscous flow ΔG^{E*} in terms of the viscosity and molar volume of the pure components:

$$ln(\eta V) = ln(\eta V)_{ideal} + \frac{\Delta G^{E*}}{RT}, \tag{10}$$

$$ln(\eta V) = \sum_{i=1}^{n} x_i ln(\eta_i V_i^0) + \frac{\Delta G^{E*}}{RT}, \tag{11}$$

where η, η_i, V, V_i^0, x_i, R, T, and ΔG^{E*} refer to the viscosity of the mixture, viscosity of pure component, molar volume of the mixture, molar volume of the pure component, mole fraction, gas constant, temperature, and excess free energy of activation for viscous flow, respectively. The subscripts are as follows: $i = 1$ for the tertiary amine, $i = 2$ for the primary amine (MEA), and $i = 3$ for H_2O.

A Redlich–Kister-type [35] polynomial, as given by Equations (12)–(14), was proposed to fit the calculated ΔG^{E*} for the considered amine mixtures:

$$\Delta G^{E*} = \Delta G_{12}^{E*} + \Delta G_{23}^{E*} + \Delta G_{13}^{E*}, \tag{12}$$

$$\Delta G_{jk}^{E*} = x_j x_k \sum_{i=0}^{n} A_i \left(x_j - x_k\right)^i, \tag{13}$$

$$A_i = a + b(T) + c(T)^2. \tag{14}$$

The correlation proposed for ΔG^{E*} was adopted to represent the measured viscosities, as illustrated in Figure 3. Due to the non-availability of measured density data beyond 343.15 K, the correlation represents viscosities only in the temperature region of 293.15 K–343.15 K. The calculated parameters of correlation for ΔG^{E*} are given in Tables 14–16. The reported *AARD* and *AMD* for the correlated viscosities of MDEA + MEA + H_2O, DMEA + MEA + H_2O, and DEEA + MEA + H_2O mixtures are listed in Table 17 and show that the proposed correlations fit viscosity data with acceptable accuracy.

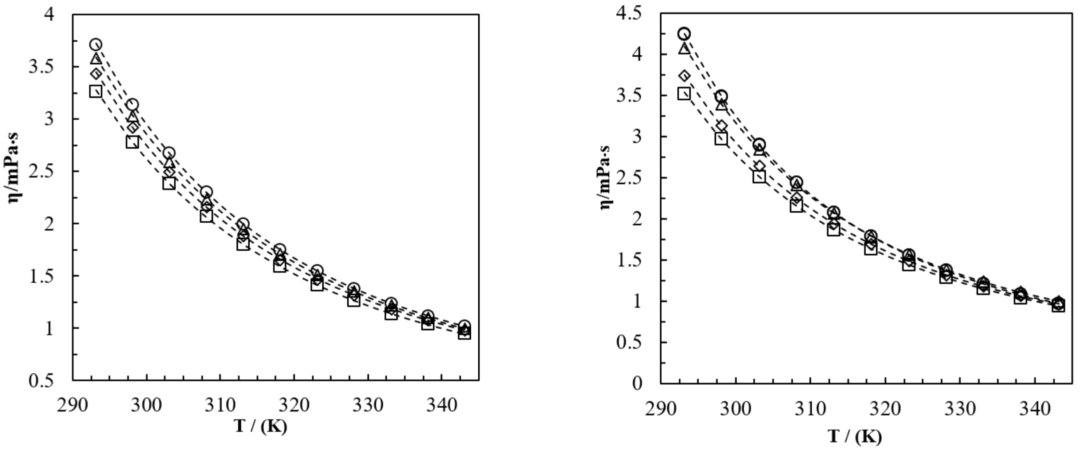

(**a**) Experiment; "□" 15%, "△" 20%, "◇" 25%, "○" 30% (mass% MDEA), correlation; "– – –".

(**b**) Experiment; "□" 15%, "△" 20%, "◇" 25%, "○" 30% (mass% DMEA), correlation; "– – –".

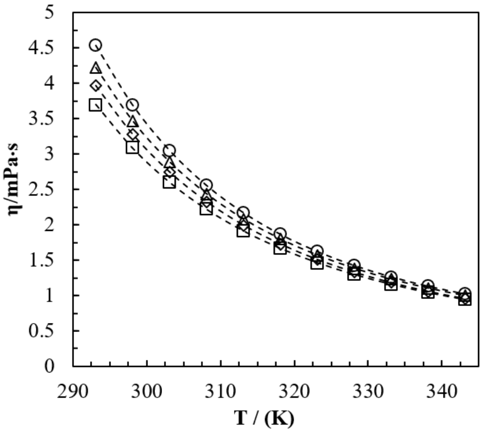

(**c**) Experiment; "□" 15%, "Δ" 20%, "◇" 25%, "○" 30% (mass% DEEA), correlation; "– – –".

Figure 3. Viscosity of: (**a**) MDEA + MEA + H_2O, (**b**) DMEA + MEA + H_2O, and (**c**) DEEA + MEA + H_2O mixtures in the temperature range 293.15 K–343.15 K.

Table 14. Binary parameters A_0, A_1, and A_2 of the equation $\Delta G_{jk}^{E*} = x_j x_k \sum_{i=0}^{n} A_i \left(x_j - x_k\right)^i$ for the excess free energy of activation for the viscous flow of MDEA (1) + MEA (2) + H_2O (3).

Parameters		**Binary Pair**		
		MDEA + MEA	**MEA + H_2O**	**MDEA + H_2O**
A_0	*a*	793,598.3561	29,742.8180	88,484.8967
	b	−4103.0875	−151.4883	−415.9737
	c	0.0695	0.9416	1.1885
A_1	*a*	−24,596,691.6004	−34,368.3693	−100,459.5203
	b	144054.1895	176.3634	472.7640
	c	−147.3226	0.1721	−0.0422
A_2	*a*	−992,156,463.1846	39,623.1737	114,056.3754
	b	6,459,639.6117	−202.4417	−536.0680
	c	−11,029.3913	0.2259	0.6852

Table 15. Binary parameters A_0, A_1, and A_2 of the equation $\Delta G_{jk}^{E*} = x_j x_k \sum_{i=0}^{n} A_i \left(x_j - x_k\right)^i$ for the excess free energy of activation for the viscous flow of DMEA (1) + MEA (2) + H_2O (3).

Parameters		**Binary Pair**		
		DMEA + MEA	**MEA + H_2O**	**DMEA + H_2O**
A_0	*a*	408,836.2339	23,045.8957	121,961.3271
	b	−2025.9328	−111.1510	−594.2230
	c	−1.7551	0.3358	1.2015
A_1	*a*	−7,605,815.8343	−26,647.3964	−142,650.2697
	b	30,647.5124	129.8558	695.9285
	c	7.3689	0.1302	−0.18829
A_2	*a*	200,073,604.4909	30,794.61597	166,795.8337
	b	−1,158,470.4621	−148.3353	−812.9574
	c	1738.2732	0.7219	1.4276

Table 16. Binary parameters A_0, A_1, and A_2 of the equation $\Delta G_{jk}^{E*} = x_j x_k \sum_{i=0}^{n} A_i \left(x_j - x_k\right)^i$ for the excess free energy of activation for the viscous flow of DEEA (1) + MEA (2) + H_2O (3).

Parameters	**Binary Pair**		
	DEEA + MEA	**MEA + H_2O**	**DEEA + H_2O**

A_0	a	25,126.2870	6568.5853	187,358.9813
	b	1235.2155	6.8875	−956.1233
	c	−1.4932	0.0215	1.6908
A_1	a	−29,279,977.3999	−6903.8084	−212,891.0602
	b	170,793.9954	−12.0764	1087.3001
	c	−281.5476	0.6502	−0.8913
A_2	a	1,130,127,942.1759	7134.8943	241,892.0192
	b	−7,848,704.4368	20.9358	−1233.8639
	c	13,825.2946	0.4399	2.0013

Table 17. Average absolute relative (*AARD*) and absolute maximum (*AMD*) deviations calculated based on correlations proposed using Equations (12)–(14).

Mixture	*AARD* (%)	*AMD* (mPa s)
MDEA + MEA + H_2O	0.14	0.013
DMEA + MEA + H_2O	0.10	0.013
DEEA + MEA + H_2O	0.07	0.010

The supplementary materials provide the information of the used MATLAB program for the calculation of parameters involve in viscosity correlation.

According to Meyer et al. [54], molecular interactions in liquid mixtures can be studied by adopting ΔG^{E*}, similar to the η^E. Studies performed in References [41,55–57] suggested that a positive deviation of ΔG^{E*} indicates strong intermolecular interactions, such as H-bonds among unlike molecules, while a negative deviation of ΔG^{E*} signifies weak molecular interactions, such as dispersive forces.

The mixtures examined in this study demonstrated positive deviations for ΔG^{E*} for the considered amine concentrations and temperatures, indicating the presence of strong intermolecular interactions like H-bonds between the molecules in the mixtures. The presence of (–OH) and (–NH_2) groups in amines contributes to the formation of H-bonds between unlike molecules. For the MDEA + MEA + H_2O mixtures, the highest ΔG^{E*} was reported for the mixture of 30 mass% MDEA + 0 mass% MEA + 70 mass% H_2O. The highest ΔG^{E*} for DEEA + MEA + H_2O was reported for the mixture of 30 mass% DEEA + 0 mass% MEA + 70 mass% H_2O, while for DMEA + MEA + H_2O, the highest ΔG^{E*} was reported for the mixture of 30 mass% DMEA + 0 mass% MEA + 70 mass% H_2O. The increases of MEA concentration gradually decreased the ΔG^{E*} for all mixtures, as shown in the Figure 4.

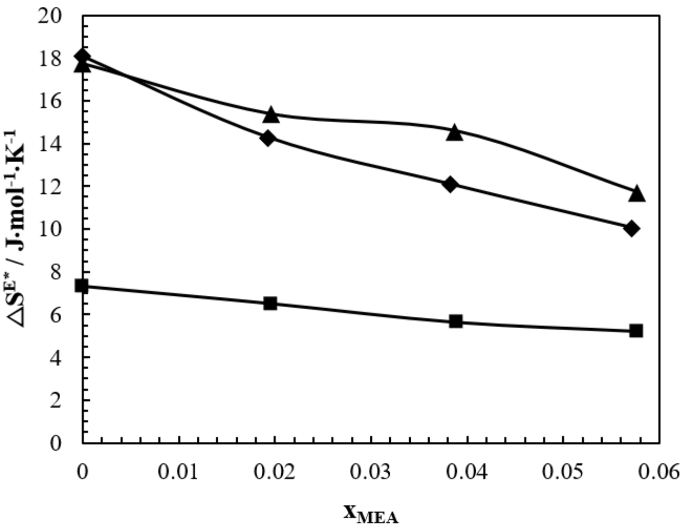

Figure 4. Excess free energy ΔG^{E*} of activation for the viscous flow of "■"—MDEA + MEA + H_2O, "◆"—DMEA + MEA + H_2O, and "▲"—DEEA + MEA + H_2O at 293.15 K.

The slope of the excess free energy of activation ΔG^{E*} against temperature T at certain mole fractions gives the excess entropy of activation ΔS^{E*} for the viscous flow:

$$\Delta S^{E*} = -\left[\frac{\partial \Delta G^{E*}}{\partial T}\right]. \tag{15}$$

Figure 5 shows the excess entropy of activation ΔS^{E*} for the viscous flow of MDEA + MEA + H_2O, DMEA + MEA + H_2O, and DEEA + MEA + H_2O in the temperature range of 293.15 K–343.15 K over the whole range of concentrations. The values for ΔS^{E*} were determined using Equation (15). Figure 5 reveals that the excess entropy ΔS^{E*} followed the same trend as ΔG^{E*}, that is, ΔS^{E*} decreased with the increase of MEA concentration in the mixture. A maximum value for ΔS^{E*} was observed at solutions with 0 mass% MEA.

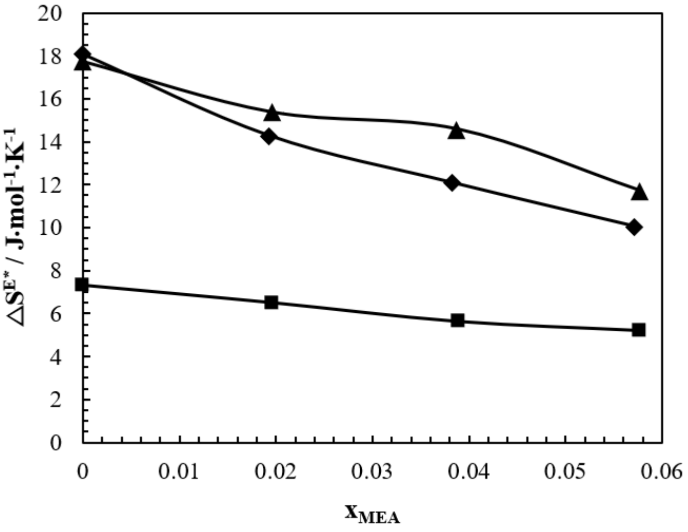

Figure 5. Excess entropy of activation ΔS^{E*} for the viscous flow of "■"—MDEA + MEA + H_2O, "◆"—DMEA + MEA + H_2O, and "▲"—DEEA + MEA + H_2O for a range of MEA mole fractions.

4. Conclusions

This paper discusses the densities and viscosities of MDEA + MEA + H_2O, DMEA + MEA + H_2O, and DEEA + MEA + H_2O mixtures at different concentrations of 15/15, 20/10, 25/5, and 30/0 for mass% (tertiary amine; MDEA, DMEA and DEEA)/mass% (primary amine; MEA) and temperatures.

The density of the mixtures was measured in the temperature range from 293.15 K to 343.15 K. The density of the mixtures increased with the increase of MDEA concentration and the density decreased with the increase of temperature for MDEA + MEA + H_2O mixtures. For the mixtures of DMEA + MEA + H_2O and DEEA + MEA + H_2O, the density decreased with the increase of DMEA and DEEA concentrations and the density decreased with the increase of temperature. The excess volume V^E of the mixtures was determined and were correlated according to a Redlich–Kister-type polynomial to represent the measured densities. A negative sign of the excess volume V^E indicates effective packing of the molecules and the presence of H-bonding among the unlike molecules. The proposed correlation was able to fit the density data with the acceptable accuracies of 0.013%, 0.004%, and 0.005% for *AARD* and 0.4 kg m^{-3}, 0.3 kg·m^{-3}, and 0.3 kg m^{-3} for *AMD* for the MDEA + MEA + H_2O, DMEA + MEA + H_2O, and DEEA + MEA + H_2O mixtures, respectively.

The viscosity of the mixtures was measured in the temperature range from 293.15 K to 363.15 K. The viscosity of the mixture increased with the increase of MDEA, DMEA, and DEEA concentration in the mixtures and the viscosity decreased with the increase of temperature. The viscosity deviation η^E was negative for the MDEA + MEA + H_2O at low temperatures, indicating weak intermolecular interactions in the mixture compared to the pure liquids. A positive η^E was reported for the DMEA + MEA + H_2O and DEEA + MEA + H_2O mixtures for the considered temperature range, signifying the presence of strong intermolecular interactions, such as H-bonds, in the mixtures. The excess free energy of activation ΔG^{E*} for viscous flow, as described by Eyring, showed positive values for all mixtures for the temperature range. This highlights the existence of strong intermolecular interactions, such as H-bonds, between the molecules in the mixtures. The correlation proposed for the calculated ΔG^{E*} from measured densities and viscosities was able to fit the ΔG^{E*} with 0.15%, 0.09%, and 0.07% for *AARD* for the MDEA + MEA + H_2O, DMEA + MEA + H_2O, and DEEA + MEA + H_2O mixtures, respectively.

Supplementary Materials: The supplementary materials are available online at www.mdpi.com/2311-5521/5/1/27/s1.

Author Contributions: Supervision, L.E.Ø., K.J.J. and D.A.E.; Writing—original draft, S.S.K.

Funding: This work was funded by the Ministry of Education and Research of the Norwegian Government.

Conflicts of Interest: The authors declare no conflict of interest.

References

1. Metz, B.; Davidson, O.; Coninck, H.D.; Loos, M.; Meyer, L. *IPCC Special Report on Carbon Dioxide Capture and Storage*; Cambridge University Press: New York, NY, USA, 2005.
2. Idem, R.; Supap, T.; Shi, H.; Gelowitz, D.; Ball, M.; Campbell, C.; Tontiwachwuthikul, P. Practical experience in post-combustion CO_2 capture using reactive solvents in large pilot and demonstration plants. *Int. J. Greenh. Gas Control* **2015**, *40*, 6–25, doi:10.1016/j.ijggc.2015.06.005.
3. Singh, A.; Stéphenne, K. Shell Cansolv CO_2 capture technology: Achievement from First Commercial Plant. *Energy Procedia* **2014**, *63*, 1678–1685, doi:10.1016/j.egypro.2014.11.177.
4. Bernhardsen, I.M.; Knuutila, H.K. A review of potential amine solvents for CO_2 absorption process: Absorption capacity, cyclic capacity and pKa. *Int. J. Greenh. Gas Control* **2017**, *61*, 27–48, doi:10.1016/j.ijggc.2017.03.021.
5. da Silva, E.F.; Svendsen, H.F. Computational chemistry study of reactions, equilibrium and kinetics of chemical CO_2 absorption. *Int. J. Greenh. Gas Control* **2007**, *1*, 151–157, doi:10.1016/S1750-5836(07)00022-9.
6. Idris, Z.; Eimer, D.A. Density measurements of unloaded and CO_2 loaded 3 - Amino -1- propanol solutions at temperatures (293.15 to 353.15) K. *J. Chem. Eng. Data* **2016**, *61*, 173–181.
7. Hartono, A.; da Silva, E.F.; Grasdalen, H.; Svendsen, H.F. Qualitative Determination of Species in DETA−H_2O−CO_2 System Using 13C NMR Spectra. *Ind. Eng. Chem. Res.* **2007**, *46*, 249–254, doi:10.1021/ie0603868.
8. Hartono, A.; Svendsen, H.F. Density, viscosity, and excess properties of aqueous solution of diethylenetriamine (DETA). *J. Chem. Thermodyn.* **2009**, *41*, 973–979, doi:10.1016/j.jct.2008.11.012.
9. Jiang, W.; Luo, X.; Gao, H.; Liang, Z.; Liu, B.; Tontiwachwuthikul, P.; Hu, X. A comparative kinetics study of CO_2 absorption into aqueous DEEA/MEA and DMEA/MEA blended solutions *Aiche J.* **2017**, *64*, 1350–1358, doi:10.1002/aic.16024.
10. Kim, I.; Svendsen, H.F. Comparative study of the heats of absorption of post-combustion CO_2 absorbents. *Int. J. Greenh. Gas Control* **2011**, *5*, 390–395, doi:10.1016/j.ijggc.2010.05.003.
11. Zhang, J.; Fennell, P.S.; Trusler, J.P.M. Density and Viscosity of Partially Carbonated Aqueous Tertiary Alkanolamine Solutions at Temperatures between (298.15 and 353.15) K. *J. Chem. Eng. Data* **2015**, *60*, 2392–2399, doi:10.1021/acs.jced.5b00282.
12. Kidnay, A.J.; Parrish, W.R. *Fundamentals of Natural Gas Processing*; Taylor & Francis Group: Boca Raton, FL, USA, 2006.
13. Jou, F.-Y.; Carroll, J.J.; Mather, A.E.; Otto, F.D. The solubility of carbon dioxide and hydrogen sulfide in a 35 wt% aqueous solution of methyldiethanolamine. *Can. J. Chem. Eng.* **1993**, *71*, 264–268, doi:10.1002/cjce.5450710213.
14. Rinker, E.B.; Sami, S.A.; Sandall, O.C. Kinetics and modelling of carbon dioxide absorption into aqueous solutions of N-methyldiethanolamine. *Chem. Eng. Sci.* **1995**, *50*, 755–768, doi:10.1016/0009-2509(94)00444-V.
15. Daviet, G.R.; Sundermann, R.; Donnelly, S.T.; Bullin, J.A. Dome's North Caroline Plant Successful Conversion to MDEA. In Proceedings of the Sixty-Third GPA Annual Convention. Available online: https://www.bre.com/PDF/Dome's-North-Caroline-Plant-Successful-Conversion-to-MDEA.pdf (accessed on 3 January 2020).

16. Blanc, C.; Grall, M.; Demarais, G. Part played by degradation products in the corrosion of gas sweetening plants using DEA and MDEA. In Proceedings of the Annual Oklahoma University gas conditioning conference, Norman, OK, USA, 8 March 1982.
17. Kim, C.J.; Savage, D.W. Kinetics of carbon dioxide reaction with diethylaminoethanol in aqueous solutions. *Chem. Eng. Sci.* **1987**, *42*, 1481–1487, doi:10.1016/0009-2509(87)85020-0.
18. Henni, A.; Li, J.; Tontiwachwuthikul, P. Reaction kinetics of CO_2 in Aqueous 1-Amino-2-Propanol, 3-Amino-1-Propanol, and Dimethylmonoethanolamine solutions in the temperature range of 298−313 K using the stopped-flow technique. *Ind. Eng. Chem. Res.* **2008**, *47*, 2213–2220, doi:10.1021/ie070587r.
19. Chakravarty, T.; Phukan, U.K.; Weilund, R.H. Reaction of Acid gases with mixtures of amines. *Chem. Eng. Prog.* **1985**, *40*, 32–36.
20. Ramachandran, N.; Aboudheir, A.; Idem, R.; Tontiwachwuthikul, P. Kinetics of the Absorption of CO_2 into Mixed Aqueous Loaded Solutions of Monoethanolamine and Methyldiethanolamine. *Ind. Eng. Chem. Res.* **2006**, *45*, 2608–2616, doi:10.1021/ie0505716.
21. Conway, W.; Bruggink, S.; Beyad, Y.; Luo, W.; Melián-Cabrera, I.; Puxty, G.; Feron, P. CO_2 absorption into aqueous amine blended solutions containing monoethanolamine (MEA), N,N-dimethylethanolamine (DMEA), N,N-diethylethanolamine (DEEA) and 2-amino-2-methyl-1-propanol (AMP) for post-combustion capture processes. *Chem. Eng. Sci.* **2015**, *126*, 446–454, doi:10.1016/j.ces.2014.12.053.
22. Glasscock, D.A.; Critchfield, J.E.; Rochelle, G.T. CO_2 absorption/desorption in mixtures of methyldiethanolamine with monoethanolamine or diethanolamine. *Chem. Eng. Sci.* **1991**, *46*, 2829–2845, doi:10.1016/0009-2509(91)85152-N.
23. Li, M.H.; Shen, K.P. Densities and solubilities of solutions of Carbon Dioxide in water+Monoethanolamine+N-Methyldiethanolamine. *J. Chem. Eng. Data* **1992**, *37*, 288–290.
24. Li, M.-H.; Lie, Y.-C. Densities and viscosities of solutions of Monoethanolamine + N-Methyldiethanolamine + water and Monoethanolamine + 2-Amino-2-methyl-1-propanol + water. *J. Chem. Eng. Data* **1994**, *39*, 444–447.
25. Hagewiesche, D.P.; Ashour, S.S.; Sandall, O.C. Solubility and Diffusivity of Nitrous Oxide in Ternary Mixtures of Water, Monoethanolamine and N-Methyldiethanolamine and Solution Densities and Viscosities. *J. Chem. Eng. Data* **1995**, *40*, 627–629, doi:10.1021/je00019a020.
26. Harvey, A.H. *Thermodynamic Properties of Water*; NIST: Boulder, CO, USA, 1998.
27. JCGM. Evaluation of measurement data—Supplement 1 to the "Guide to the expression of uncertainty in measurement"—Propagation of distributions using a Monte Carlo method. Available online: https://www.bipm.org/utils/common/documents/jcgm/JCGM_101_2008_E.pdf (accessed on 3 January 2020).
28. Ellison, S.L.R.; Williams, A. *Quantifying Uncertainty in Analytical Measurement.* Available online: https://www.eurachem.org/images/stories/Guides/pdf/QUAM2012_P1.pdf (accessed on 3 January 2020).
29. Pinto, D.D.D.; Monteiro, J.G.M.S.; Johnsen, B.; Svendsen, H.F.; Knuutila, H. Density measurements and modelling of loaded and unloaded aqueous solutions of MDEA (N-methyldiethanolamine), DMEA (N,N-dimethylethanolamine), DEEA (diethylethanolamine) and MAPA (N-methyl-1,3-diaminopropane). *Int. J. Greenh. Gas Control* **2014**, *25*, 173–185, doi:10.1016/j.ijggc.2014.04.017.
30. Hawrylak, B.; Bruke, S.E.; Palepu, R. Partial molar and excess volumes and adiabatic compressibilities of binary mixtures of ethanolamines with water. *J. Solut. Chem.* **2000**, *29*, 575–593.
31. Maham, Y.; Teng, T.T.; Mather, A.E.; Hepler, L.G. Volumetric properties of (water + diethanolamine) systems. *Can. J. Chem* **1995**, *73*, 1514–1519.
32. Maham, Y.; Lebrette, L.; Mather, A.E. Viscosities and Excess Properties of Aqueous Solutions of Mono- and Diethylethanolamines at Temperatures between 298.15 and 353.15 K. *J. Chem. Eng. Data* **2002**, *47*, 550–553, doi:10.1021/je015528d.
33. Bernal-García, J.M.; Hall, K.R.; Estrada-Baltazar, A.; Iglesias-Silva, G.A. Density and viscosity of aqueous solutions of N,N-dimethylethanolamine at p=0.1 MPa from T=(293.15 to 363.15) K. *J. Chem. Thermodyn.* **2005**, *37*, 762–767, doi:10.1016/j.jct.2004.11.016.
34. Zhang, F.-Q.; Li, H.-P.; Dai, M.; Zhao, J.-P.; Chao, J.P. Volumetric properties of binary mixtures of water with ethanolamine alkyl derivatives. *Thermochim. Acta* **1995**, *254*, 347–357, doi:10.1016/0040-6031(94)02127-A.

35. Redlich, O.; Kister, A.T. Algebraic representation of thermodynamic properties and the classification of solutions. *Ind. Eng. Chem.* **1948**, *40*, 345–348.
36. Domínguez, M.; Rodríguez, S.; López, M.C.; Royo, F.M.; Urieta, J.S. Densities and Viscosities of the Ternary Mixtures 1-Butanol + 1-Chlorobutane + 1-Butylamine and 2-Methyl-1-propanol + 1-Chlorobutane + 1-Butylamine at 298.15 K. *J. Chem. Eng. Data* **1996**, *41*, 37–42, doi:10.1021/je950113b.
37. Samanta, A.; Bandyopadhyay, S.S. Density and Viscosity of Aqueous Solutions of Piperazine and (2-Amino-2-methyl-1-propanol + Piperazine) from 298 to 333 K. *J. Chem. Eng. Data* **2006**, *51*, 467–470, doi:10.1021/je050378i.
38. Hartono, A.; Mba, E.O.; Svendsen, H.F. Physical properties of partially CO_2 loaded aqueous monoethanolamine (MEA). *J. Chem. Eng. Data* **2014**, *59*, 1808–1816.
39. Weiland, R.H.; Dingman, J.C.; Cronin, D.B.; Browning, G.J. Density and viscosity of some partially carbonated aqueous alkanolamine solutions and their blends. *J. Chem. Eng. Data* **1998**, *43*, 378–382.
40. Moioli, S.; Pellegrini, L.A. Physical properties of PZ solution used as a solvent for CO_2 removal. *Chem. Eng. Res. Des.* **2015**, *93*, 720–726, doi:10.1016/j.cherd.2014.06.016.
41. Bhatia, S.C.; Bhatia, R.; Dubey, G.P. Studies on transport and thermodynamic properties of binary mixtures of octan-1-ol with chloroform, 1,2-dichloroethane and 1,1,2,2-tetrachloroethane at 298.15 and 308.15 K. *J. Mol. Liq.* **2009**, *144*, 163–171, doi:10.1016/j.molliq.2008.11.003.
42. Ma, D.; Liu, Q.; Zhu, C.; Feng, H.; Ma, Y. Volumetric and viscometric properties of ternary solution of (N-methyldiethanolamine + monoethanolamine + ethanol). *J. Chem. Thermodyn.* **2019**, *134*, 5–19, doi:10.1016/j.jct.2019.02.019.
43. Teng, T.T.; Maham, Y.; Hepler, L.G.; Mather, A.E. Viscosity of aqueous solutions of N-Methyldiethanolamine and of Diethanolamine. *J. Chem. Eng. Data* **1994**, *39*, 290–293.
44. Kummamuru, N.B.; Idris, Z.; Eimer, D.A. Viscosity Measurement and Correlation of Unloaded and CO_2-Loaded Aqueous Solutions of N-Methyldiethanolamine-Piperazine. *J. Chem. Eng. Data* **2019**, doi:10.1021/acs.jced.9b00021.
45. Chowdhury, F.I.; Akhtar, S.; Saleh, M.A.; Khandaker, M.U.; Amin, Y.M.; Arof, A.K. Volumetric and viscometric properties of aqueous solutions of some monoalkanolamines. *J. Mol. Liq.* **2016**, *223*, 299–314, doi:10.1016/j.molliq.2016.08.033.
46. DiGuilio, R.M.; Lee, R.J.; Schaeffer, S.T.; Brasher, L.L.; Teja, A.S. Densities and viscosity of the ethanolamines *J. Chem. Eng.* **1992**, *37*, 239–242.
47. Chen, S.; Zhang, L.; Zhang, Y.; Chen, S.; Chen, J. Density and viscosity of monoethylethanolamine+H_2O and monoethylethanolamine+diethylethanolamine solutions for CO_2 capture. *Thermochim. Acta* **2016**, *642*, 52–58, doi:10.1016/j.tca.2016.08.021.
48. Ma, D.; Zhu, C.; Fu, T.; Yuan, X.; Ma, Y. Volumetric and viscometric properties of binary and ternary mixtures of monoethanolamine, 2-(diethylamino) ethanol and water from (293.15 to 333.15) K. *J. Chem. Thermodyn.* **2019**, *138*, 350–365, doi:10.1016/j.jct.2019.06.032.
49. Fort, R.J.; Moore, W.R. Viscosities of binary liquid mixtures. *Trans. Faraday Soc.* **1966**, *62*, 1112–1119.
50. Domínguez, M.; Camacho, A.; López, M.C.; Royo, F.M.; Urieta, J.S. Excess molar volumes and excess viscosities of ternary mixtures (2-butanol + 1-chlorobutane + 1-butylamine) and (2-methyl-2-propanol + 1-chlorobutane + 1-butylamine) at 298. 15 K. *Can. J. Chem.* **1995**, *73*, 896–901, doi:10.1139/v95-112.
51. Rafiee, H.R.; Ranjbar, S.; Poursalman, F. Densities and viscosities of binary and ternary mixtures of cyclohexanone, 1,4-dioxane and isooctane from T=(288.15 to 313.15)K. *J. Chem. Thermodyn.* **2012**, *54*, 266–271, doi:10.1016/j.jct.2012.05.005.
52. Eyring, H. Viscosity, Plasticity, and Diffusion as example of absolute reaction rates. *J. Chem. Phys.* **1936**, *4*, 283–291.
53. Bird, R.B.; Stewart, W.E.; Lightfoot, E.N. *Transport PHENOMENA*, 2nd ed.; John Wiley & Sons, Inc.: Hoboken, NJ, USA, 2002.
54. Meyer, R.; Meyer, M.; Metzger, J.; Peneloux, A. Thermodynamic and physicochemical properties of binary solvent. *J. Chim. Phys. Phys. Chim. Biol.* **1971**, *68*, 406–412.
55. Domínguez, M.; Pardo, J.I.; Gascón, I.; Royo, F.M.; Urieta, J.S. Viscosities of the ternary mixture (2-butanol+n-hexane+1-butylamine) at 298.15 and 313.15 K. *Fluid Phase Equilibria* **2000**, *169*, 277–292, doi:10.1016/S0378-3812(00)00332-0.

56. Kinart, C.M.; Kinart, W.J.; Ćwiklińska, A. 2-Methoxyethanol–Tetrahydrofuran–Binary Liquid System. Viscosities, densities, excess molar volumes and excess Gibbs activation energies of viscous flow at various temperatures. *J. Therm. Anal. Calorim.* **2002**, *68*, 307–317, doi:10.1023/A:1014981921097.
57. Ćwiklińska, A.; Kinart, C.M. Thermodynamic and physicochemical properties of binary mixtures of nitromethane with {2-methoxyethanol+2-butoxyethanol} systems at T=(293.15, 298.15, 303.15, 308.15, and 313.15)K. *J. Chem. Thermodyn.* **2011**, *43*, 420–429, doi:10.1016/j.jct.2010.10.016.